

## Supplementary Material

### Transition matrices for the simplified six-subunit model of the CaMKII autophosphorylation

This model does not take the T305 phosphorylation into account. It is presented here as a basis for the six-subunit CaMKII autophosphorylation model (that includes the T305 phosphorylation). The transition matrices  $Q_{aa}$  and  $Q_{ap}$  denote the number of ways that the autophosphorylations by active non-phospho and phospho subunits, respectively, can occur. The matrices are determined directly from the weights associated with these transitions (Figure 4A) so that the element in column  $i$  and row  $j$  of a transition matrix represents the transition from state  $j$  to  $i$ . The conservation of CaMKII requires that the diagonal elements are determined so that the sum of elements in each column is 0. All other elements are 0 (represented by dots). The complete matrices are given below:

$$\begin{aligned}
 Q_{aa} &= \begin{pmatrix} -6 & \cdot & \cdot & \cdot & \cdot & \cdot & \cdot & \cdot & \cdot & \cdot & \cdot & \cdot & \cdot & \cdot & \cdot \\ 6 & -4 & \cdot & \cdot & \cdot & \cdot & \cdot & \cdot & \cdot & \cdot & \cdot & \cdot & \cdot & \cdot & \cdot \\ \cdot & 1 & -3 & \cdot & \cdot & \cdot & \cdot & \cdot & \cdot & \cdot & \cdot & \cdot & \cdot & \cdot & \cdot \\ \cdot & 2 & \cdot & -2 & \cdot & \cdot & \cdot & \cdot & \cdot & \cdot & \cdot & \cdot & \cdot & \cdot & \cdot \\ \cdot & 1 & \cdot & \cdot & -2 & \cdot & \cdot & \cdot & \cdot & \cdot & \cdot & \cdot & \cdot & \cdot & \cdot \\ \cdot & \cdot & 1 & \cdot & \cdot & -2 & \cdot & \cdot & \cdot & \cdot & \cdot & \cdot & \cdot & \cdot & \cdot \\ \cdot & \cdot & 1 & 1 & \cdot & \cdot & -1 & \cdot & \cdot & \cdot & \cdot & \cdot & \cdot & \cdot & \cdot \\ \cdot & \cdot & \cdot & 1 & 2 & \cdot & \cdot & -1 & \cdot & \cdot & \cdot & \cdot & \cdot & \cdot & \cdot \\ \cdot & \cdot & \cdot & \cdot & 1 & \cdot & \cdot & \cdot & \cdot & \cdot & \cdot & \cdot & \cdot & \cdot & \cdot \\ \cdot & \cdot & \cdot & \cdot & \cdot & 1 & \cdot & \cdot & -1 & \cdot & \cdot & \cdot & \cdot & \cdot & \cdot \\ \cdot & \cdot & \cdot & \cdot & \cdot & 1 & 1 & \cdot & \cdot & \cdot & \cdot & \cdot & \cdot & \cdot & \cdot \\ \cdot & \cdot & \cdot & \cdot & \cdot & \cdot & \cdot & 1 & \cdot & \cdot & \cdot & \cdot & \cdot & \cdot & \cdot \\ \cdot & \cdot & \cdot & \cdot & \cdot & \cdot & \cdot & \cdot & \cdot & 1 & \cdot & \cdot & \cdot & \cdot & \cdot \\ \cdot & \cdot & \cdot & \cdot & \cdot & \cdot & \cdot & \cdot & \cdot & \cdot & 1 & \cdot & \cdot & \cdot & \cdot \\ \cdot & \cdot & \cdot & \cdot & \cdot & \cdot & \cdot & \cdot & \cdot & \cdot & \cdot & 1 & \cdot & \cdot & \cdot \\ \cdot & \cdot & \cdot & \cdot & \cdot & \cdot & \cdot & \cdot & \cdot & \cdot & \cdot & \cdot & 1 & \cdot & \cdot \end{pmatrix} \\
 Q_{ap} &= \begin{pmatrix} \cdot & \cdot & \cdot & \cdot & \cdot & \cdot & \cdot & \cdot & \cdot & \cdot & \cdot & \cdot & \cdot & \cdot & \cdot \\ \cdot & -1 & \cdot & \cdot & \cdot & \cdot & \cdot & \cdot & \cdot & \cdot & \cdot & \cdot & \cdot & \cdot & \cdot \\ \cdot & 1 & -1 & \cdot & \cdot & \cdot & \cdot & \cdot & \cdot & \cdot & \cdot & \cdot & \cdot & \cdot & \cdot \\ \cdot & \cdot & \cdot & -2 & \cdot & \cdot & \cdot & \cdot & \cdot & \cdot & \cdot & \cdot & \cdot & \cdot & \cdot \\ \cdot & \cdot & \cdot & \cdot & -2 & \cdot & \cdot & \cdot & \cdot & \cdot & \cdot & \cdot & \cdot & \cdot & \cdot \\ \cdot & \cdot & 1 & 1 & \cdot & -1 & \cdot & \cdot & \cdot & \cdot & \cdot & \cdot & \cdot & \cdot & \cdot \\ \cdot & \cdot & \cdot & \cdot & 2 & \cdot & -2 & \cdot & \cdot & \cdot & \cdot & \cdot & \cdot & \cdot & \cdot \\ \cdot & \cdot & \cdot & 1 & \cdot & \cdot & \cdot & -2 & \cdot & \cdot & \cdot & \cdot & \cdot & \cdot & \cdot \\ \cdot & \cdot & \cdot & \cdot & \cdot & \cdot & \cdot & \cdot & -3 & \cdot & \cdot & \cdot & \cdot & \cdot & \cdot \\ \cdot & \cdot & \cdot & \cdot & \cdot & 1 & 1 & 1 & \cdot & -1 & \cdot & \cdot & \cdot & \cdot & \cdot \\ \cdot & \cdot & \cdot & \cdot & \cdot & \cdot & \cdot & 1 & 3 & \cdot & -2 & \cdot & \cdot & \cdot & \cdot \\ \cdot & \cdot & \cdot & \cdot & \cdot & \cdot & 1 & \cdot & \cdot & \cdot & \cdot & -2 & \cdot & \cdot & \cdot \\ \cdot & \cdot & \cdot & \cdot & \cdot & \cdot & \cdot & \cdot & \cdot & 1 & 2 & 2 & -1 & \cdot & \cdot \\ \cdot & \cdot & \cdot & \cdot & \cdot & \cdot & \cdot & \cdot & \cdot & \cdot & \cdot & \cdot & 1 & \cdot & \cdot \end{pmatrix} \quad (\text{Eq. S1})
 \end{aligned}$$

### Transition matrices for the six-subunit model of the CaMKII autophosphorylation

These transition matrices take into account all possible transitions between the 38 states that are distinguished by the arrangement of T286 and T305 phosphorylates subunits. Each transition weight from Eq. S1 becomes a matrix here. Therefore, the transition matrices  $Q_{aa}$ ,  $Q_{ap}$ ,  $Q_{app}$ , and  $Q_{pp}$  can be represented as 14x14 block matrices. For example, the transitions from state 2 to 4 and from 7 to 12 of the simplified model (see Figure 4A, or Eq. S1) correspond to the transitions shown in Figure 4B,C, and are specified by  $(Q_{aa})_{42}$ ,  $(Q_{ap})_{127}$  and  $(Q_{app})_{127}$  given in Eq. S2 - Eq. S4.

The transition matrices  $Q_{aa}$ ,  $Q_{ap}$ , and  $Q_{app}$  are obtained by setting the individual blocks to the values given below (Eq. S2 - Eq. S4), and by setting the diagonal elements so that the elements of each column sum up to 0. All other elements are 0. As above, 0's are represented by dots.

Non-zero blocks of  $Q_{aa}$  are:

$$\begin{aligned}
 (Q_{aa})_{21} &= \begin{pmatrix} 6 \\ \cdot \end{pmatrix} & (Q_{aa})_{32} &= (Q_{aa})_{63} &= (Q_{aa})_{106} &= (Q_{aa})_{1311} &= \begin{pmatrix} 1 & \cdot \\ \cdot & 1 \end{pmatrix} \\
 (Q_{aa})_{52} &= \begin{pmatrix} 1 & \cdot \\ \cdot & 1 \\ \cdot & \cdot \end{pmatrix} & (Q_{aa})_{73} &= (Q_{aa})_{83} &= (Q_{aa})_{116} &= \begin{pmatrix} 1 & \cdot \\ \cdot & 1 \\ \cdot & \cdot \end{pmatrix} \\
 (Q_{aa})_{42} &= \begin{pmatrix} 2 & \cdot \\ \cdot & 1 \\ \cdot & 1 \\ \cdot & \cdot \end{pmatrix} & (Q_{aa})_{74} &= (Q_{aa})_{94} &= (Q_{aa})_{117} &= \begin{pmatrix} 1 & \cdot & \cdot & \cdot \\ \cdot & 1 & \cdot & \cdot \\ \cdot & \cdot & 1 & \cdot \\ \cdot & \cdot & \cdot & 1 \end{pmatrix}
 \end{aligned}$$

$$(Q_{aa})_{85} = \begin{pmatrix} 2 & \cdot & \cdot \\ \cdot & 1 & \cdot \\ \cdot & 1 & \cdot \\ \cdot & \cdot & 2 \end{pmatrix} \quad (Q_{aa})_{128} = \begin{pmatrix} 1 & \cdot & \cdot & \cdot \\ \cdot & 1 & 1 & \cdot \\ \cdot & \cdot & \cdot & 1 \end{pmatrix} \quad (\text{Eq. S2})$$

Non-zero blocks of matrices  $Q_{ap}$  are:

$$\begin{aligned} (Q_{ap})_{32} &= (Q_{ap})_{63} = (Q_{ap})_{106} = (Q_{ap})_{1310} = \begin{pmatrix} 1 & \cdot \\ \cdot & \cdot \end{pmatrix} \\ (Q_{ap})_{64} &= (Q_{ap})_{107} = \begin{pmatrix} 1 & \cdot & \cdot & \cdot \\ \cdot & \cdot & 1 & \cdot \end{pmatrix} \quad (Q_{ap})_{84} = \begin{pmatrix} 1 & \cdot & \cdot & \cdot \\ \cdot & 1 & \cdot & \cdot \\ \cdot & \cdot & \cdot & \cdot \end{pmatrix} \\ (Q_{ap})_{75} &= \begin{pmatrix} 2 & \cdot & \cdot \\ \cdot & \cdot & \cdot \\ \cdot & 1 & \cdot \\ \cdot & \cdot & \cdot \end{pmatrix} \quad (Q_{ap})_{127} = \begin{pmatrix} 1 & \cdot & \cdot & \cdot \\ \cdot & 1 & \cdot & \cdot \\ \cdot & \cdot & \cdot & \cdot \end{pmatrix} \\ (Q_{ap})_{108} &= \begin{pmatrix} 1 & \cdot & \cdot & \cdot \\ \cdot & 1 & \cdot & \cdot \end{pmatrix} \quad (Q_{ap})_{118} = \begin{pmatrix} 1 & \cdot & \cdot & \cdot \\ \cdot & \cdot & \cdot & \cdot \\ \cdot & \cdot & 1 & \cdot \\ \cdot & \cdot & \cdot & \cdot \end{pmatrix} \\ (Q_{ap})_{119} &= \begin{pmatrix} 3 & \cdot & \cdot & \cdot \\ \cdot & 1 & \cdot & \cdot \\ \cdot & 1 & \cdot & \cdot \\ \cdot & \cdot & 1 & \cdot \end{pmatrix} \quad (Q_{ap})_{1311} = \begin{pmatrix} 2 & \cdot & \cdot & \cdot \\ \cdot & 1 & 1 & \cdot \end{pmatrix} \\ (Q_{ap})_{1312} &= \begin{pmatrix} 2 & \cdot & \cdot \\ \cdot & 1 & \cdot \end{pmatrix} \quad (Q_{ap})_{1413} = (1 \ \cdot) \end{aligned} \quad (\text{Eq. S3})$$

Non-zero blocks of matrices  $Q_{app}$  are:

$$\begin{aligned} (Q_{app})_{32} &= (Q_{app})_{63} = (Q_{app})_{106} = (Q_{app})_{1310} = \begin{pmatrix} \cdot & 1 \\ \cdot & \cdot \end{pmatrix} \\ (Q_{app})_{64} &= (Q_{app})_{107} = \begin{pmatrix} \cdot & 1 & \cdot & \cdot \\ \cdot & \cdot & \cdot & 1 \end{pmatrix} \quad (Q_{app})_{84} = \begin{pmatrix} \cdot & \cdot & 1 & \cdot \\ \cdot & \cdot & \cdot & \cdot \\ \cdot & \cdot & \cdot & 1 \\ \cdot & \cdot & \cdot & \cdot \end{pmatrix} \\ (Q_{app})_{75} &= \begin{pmatrix} \cdot & 1 & \cdot \\ \cdot & \cdot & \cdot \\ \cdot & \cdot & 2 \\ \cdot & \cdot & \cdot \end{pmatrix} \quad (Q_{app})_{127} = \begin{pmatrix} \cdot & \cdot & 1 & \cdot \\ \cdot & \cdot & \cdot & 1 \\ \cdot & \cdot & \cdot & \cdot \end{pmatrix} \\ (Q_{app})_{108} &= \begin{pmatrix} \cdot & \cdot & 1 & \cdot \\ \cdot & \cdot & \cdot & 1 \end{pmatrix} \quad (Q_{app})_{118} = \begin{pmatrix} \cdot & 1 & \cdot & \cdot \\ \cdot & \cdot & \cdot & \cdot \\ \cdot & \cdot & \cdot & 1 \\ \cdot & \cdot & \cdot & \cdot \end{pmatrix} \\ (Q_{app})_{119} &= \begin{pmatrix} \cdot & 1 & \cdot & \cdot \\ \cdot & \cdot & 1 & \cdot \\ \cdot & \cdot & 1 & \cdot \\ \cdot & \cdot & \cdot & 3 \end{pmatrix} \quad (Q_{app})_{1311} = \begin{pmatrix} \cdot & 1 & 1 & \cdot \\ \cdot & \cdot & \cdot & 2 \end{pmatrix} \\ (Q_{app})_{1312} &= \begin{pmatrix} \cdot & 1 & \cdot \\ \cdot & \cdot & 2 \end{pmatrix} \quad (Q_{app})_{1413} = (\cdot \ 1) \end{aligned} \quad (\text{Eq. S4})$$

The transition matrix  $Q_{pp}$ , corresponding to the phosphorylation at T305, is obtained by setting the individual blocks to the values given below (Eq. S5), and by setting all other elements to 0. Only the diagonal blocks contain non-zero elements.

$$\begin{aligned} (Q_{pp})_{22} &= (Q_{pp})_{33} = (Q_{pp})_{66} = (Q_{pp})_{1010} = (Q_{pp})_{1313} = \begin{pmatrix} -1 & \cdot \\ 1 & \cdot \end{pmatrix} \\ (Q_{pp})_{44} &= (Q_{pp})_{77} = (Q_{pp})_{88} = (Q_{pp})_{1111} = \begin{pmatrix} -2 & \cdot & \cdot & \cdot \\ 1 & -1 & \cdot & \cdot \\ 1 & \cdot & -1 & \cdot \\ \cdot & 1 & 1 & \cdot \end{pmatrix} \quad (\text{Eq. S5}) \\ (Q_{pp})_{55} &= (Q_{pp})_{1212} = \begin{pmatrix} -2 & \cdot & \cdot \\ 2 & -1 & \cdot \\ \cdot & 1 & \cdot \end{pmatrix} \quad (Q_{pp})_{99} = \begin{pmatrix} -3 & \cdot & \cdot & \cdot \\ 3 & -2 & \cdot & \cdot \\ \cdot & 2 & -1 & \cdot \\ \cdot & \cdot & 1 & \cdot \end{pmatrix} \end{aligned}$$

## Experimental methods

Cation	Ligand	T = 25 <sup>o</sup> C			T = 30 <sup>o</sup> C	
		log K	log K	$\Delta H$ [kJ/mol]	log K	log K
		no H <sup>+</sup>	pH 7.1		no H <sup>+</sup>	pH 7.1
H <sup>+</sup>	EGTA <sup>4-</sup>	9.40		-24	9.33	
H <sup>+</sup>	H EGTA <sup>3-</sup>	8.78		-24	8.71	
Ca <sup>2+</sup>	EGTA <sup>4-</sup>	10.86	6.87	-34	10.76	6.91
Mg <sup>2+</sup>	EGTA <sup>4-</sup>	5.28	1.29	21	5.34	1.49

Table S1: EGTA binding constants for Ca<sup>2+</sup>, Mg<sup>2+</sup> and H<sup>+</sup>. Log values of EGTA affinities for H<sup>+</sup>, Ca<sup>2+</sup> and Mg<sup>2+</sup>, and of EGTA affinities for Ca<sup>2+</sup> and Mg<sup>2+</sup> at pH 7.1, at 25 and 30°C.  $\Delta H$  is the enthalpy of the complexes formed by these bindings.

total Ca <sup>2+</sup> [ $\mu M$ ]	free Ca <sup>2+</sup> [ $\mu M$ ]								
	T	25°C				30°C			
	CaM	-	+	+	+	-	+	+	+
	CaMKII	-	-	+P286	average	-	-	+P286	average
352.6		1.00	0.99	0.98	0.99	0.92	0.91	0.90	0.91
368.4		1.52	1.50	1.48	1.49	1.40	1.39	1.36	1.37
378.9		2.22	2.16	2.12	2.14	2.05	2.01	1.97	1.99
389.5		3.72	3.53	3.42	3.47	3.48	3.31	3.21	3.26
394.7		5.12	4.74	4.57	4.65	4.84	4.48	4.32	4.40

Table S2: Free Ca<sup>2+</sup> concentrations for our experimental conditions. Free Ca<sup>2+</sup> was calculated for both 25°C and 30°C, for different cases involving the presence and absence of CaM and CaMKII 100% autophosphorylated at T286. The values in the fourth (“average”) columns were obtained from the preceding two columns. The concentrations of CaM and CaMKII used were the same as in our CaMKII autophosphorylation assay.

## CaMKII autophosphorylation measurements

T [°C]	free Ca <sup>2+</sup> [ $\mu M$ ]	P286				P305	
		30 s	60 s	120 s	180 s	120 s	180 s
25	0.99				< 0.1		
	1.49	0.03±0.03	0.18±0.14	0.31±0.20	0.41±0.18	0.03±0.03	0.04±0.03
	2.14	0.43±0.16	0.64±0.16	0.74±0.11	0.85±0.09	0.08±0.04	0.16±0.06
	3.47	0.81±0.01	0.93±0.01	0.94±0.01	0.96±0.01	0.16±0.04	0.26±0.04
	4.65	> 0.9					0.3
30	1.37	0.17±0.14	0.45±0.17	0.68±0.11	0.75±0.12	0.24±0.08	0.42±0.10
	1.99	0.66±0.05	0.85±0.01	0.91±0.02	0.93±0.02	0.45±0.06	0.68±0.05
	3.26	0.90±0.02	0.95±0.002	0.96±0.01	0.97±0.01	0.56±0.04	0.71±0.05

Table S3: Experimentally determined  $\alpha$ CaMKII autophosphorylation data. Amounts of  $\alpha$ CaMKII autophosphorylated at T286 (obtained from anti non-phospho T286  $\alpha$ CaMKII Westerns) and T286 (anti-phospho T286 CaMKII Westerns), normalized so that the total  $\alpha$ CaMKII has a value of 1, are given for different temperatures, free Ca<sup>2+</sup> concentrations, and reaction times.

## Simulations: Six-subunit model of CaMKII autophosphorylation

T [°C]	Free Ca <sup>2+</sup> [μM]	Two-phospho rates						One-phospho rate						$k_{eff}^{PPP}$ [s <sup>-1</sup> ]
		$r_{\alpha}^{(0)}$			$r_{\alpha}$			$r_{\alpha}$ (Fast)			$r_{\alpha}$ (Slow)			
		min	best	max	min	best	max	min	best	max	min	best	max	
25	0.99			0.02			0.0066			0.0038			0.017	
	1.49	0.024	0.045	0.07	0.0076	0.014	0.022	0.005	0.008	0.012	0.022	0.036	0.049	0.0013
	2.14	0.11	0.15	0.24	0.034	0.047	0.076	0.017	0.019	0.024	0.080	0.088	0.098	0.0015
	3.47	0.5	0.6	0.8	0.16	0.19	0.25	0.037	0.039	0.041	0.18	0.19	0.21	0.0019
	4.65	1			0.32			0.046			0.24			<0.002
30	1.37	0.06	0.09	0.12	0.011	0.016	0.022	0.008	0.010	0.013	0.034	0.045	0.058	0.007
	1.99	0.2	0.23	0.26	0.036	0.042	0.047	0.019	0.021	0.023	0.09	0.10	0.11	0.009
	3.26	0.4	0.5	0.8	0.073	0.091	0.15	0.029	0.032	0.036	0.13	0.15	0.17	0.008

Table S4: Results of the parameter search using the six-subunit CaMKII autophosphorylation model. Values of normalized (and real) probability  $r_{\alpha}^{(0)}$  ( $r_{\alpha}$ ), and  $k_{eff}^{PPP}$  for one-phospho and two-phospho rates six-subunit CaMKII autophosphorylation models that provided the best fit to the experimental data are given for different temperature and free Ca<sup>2+</sup>. The lower and upper limits of parameter  $r_{\alpha}^{(0)}$  that provided acceptable fits are given in columns min and max respectively. In the case of the two-phospho rates variant, the normalized parameter  $k_{ap}^{P(0)}$  was 0.05 s<sup>1/2</sup> (25°C) and 0.10 s<sup>1/2</sup> (30°C),. Real probability  $r_{\alpha}$  was obtained using the fast phosphorylation values of  $k_{aa}^P$  given in Table S5. In the one-phospho rates variant, two available estimates of the T286 phosphorylation rate  $k_{aa}^P$  were used to define the fast (6.3/s at 25°C and 11.9 /s at 30°C) and the slow (0.53/s at 25°C and 1/s at 30°C) phosphorylation rate variants.

T [°C]	Fast phosphorylation			Slow phosphorylation		
	Two-phospho rates	One-phospho rate		Two-phospho rates	One-phospho rate	
	$k_{aa}^P$ [1/s]	$k_{ap}^P$ [1/s]	$k_{aa}^P = k_{ap}^P$ [1/s]	$k_{aa}^P$ [1/s]	$k_{ap}^P$ [1/s]	$k_{aa}^P = k_{ap}^P$ [1/s]
25	10	0.16	6.3	1.6	0.063	0.53
30	30	0.55	11.9	2.2	0.15	1

Table S5: Values for the phosphorylation rates at T286.

The values in fast phosphorylation / one-phospho rate column are taken from (Bradshaw et al. 2003) and those in slow phosphorylation / one-phospho rate column (at 30°C) from (Miller and Kennedy 1986; Hanson et al. 1994). The values of  $k_{aa}^P$  and  $k_{ap}^P$  given in the two-phospho rates columns are the best fit values obtained using the two-phospho rates model.

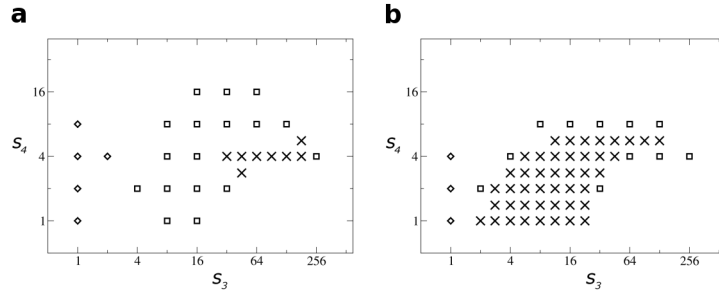


Figure S1: Affinity increase parameters  $s_3$  and  $s_4$ .

Values of  $s_3$  and  $s_4$  that were consistent with our experimental data for the 3-activation,  $1/K_{\alpha 4} = 20\text{nM}$ , fast phosphorylation variant in combination with two-phospho rate variants are indicated by X symbol. Symbols  $\diamond$  and  $\square$  show  $s_3$  and  $s_4$  satisfying the relaxed conditions for one- and two-phospho variants, respectively. (A) Results for  $25^\circ\text{C}$ , (B) Results for  $30^\circ\text{C}$ .

### Simulations: The complete dynamic model

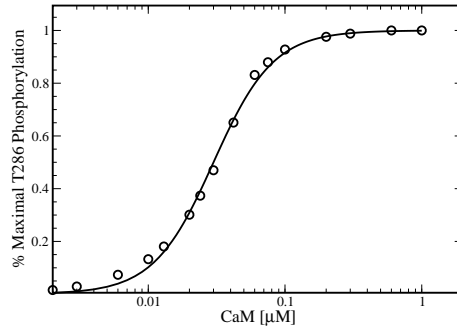


Figure S2: T286 phosphorylation dependence on  $[\text{CaM}]$  in saturating  $\text{Ca}^{2+}$  fit to the Hill equation. Simulation results for the T286 phosphorylation of  $\alpha\text{CaMKII}$  in saturating  $\text{Ca}^{2+}$  obtained using the complete dynamic model with 2-phospho, fast, 3-activation variant combination, without T305 phosphorylation are shown with circles. The parameters were:  $[\alpha\text{CaMKII}] = 70\text{ nM}$ ,  $k_{aa}^P = 10/s$ ,  $k_{ap}^P = 0.16/s$ ,  $1/K_{\alpha 4} = 20\text{ nM}$ ,  $[\text{Ca}] = 500\text{ }\mu\text{M}$ ,  $s_1 = s_2 = s_4 = 1$ ,  $s_3 = 16$  (the exact  $s$  values are irrelevant because  $\text{Ca}^{2+}$  is saturating). The simulation results were fit with the Hill equation:  $y = x^h / (x^h + K_D^h)$ . The best-fit curve was obtained for Hill coefficient ( $h$ ) of 2.0 and  $K_D = 30\text{ nM}$ .

## Simulations: Two-subunit model of CaMKII autophosphorylation

T [°C]	Free Ca <sup>2+</sup> [μM]	Two-phospho rates						One-phospho rate						$k_{eff}^{PP}$ [s <sup>-1</sup> ]
		$r_{\alpha}^{(0)}$			$r_{\alpha}$			$r_{\alpha}$ (Fast)			$r_{\alpha}$ (Slow)			
		min	best	max	min	best	max	min	best	max	min	best	max	
25	0.99			0.019			0.006			0.055			0.020	
	1.49	0.025	0.046	0.072	0.0079	0.015	0.023	0.007	0.013	0.018	0.026	0.046	0.065	0.0013
	2.14	0.11	0.17	0.29	0.035	0.54	0.092	0.025	0.030	0.038	0.090	0.108	0.136	0.0015
	3.47	0.64	0.76	0.93	0.20	0.24	0.29	0.057	0.061	0.065	0.205	0.22	0.24	0.0019
	4.65	1.24			0.39			0.075			0.28			<0.002
30	1.37	0.062	0.084	0.118	0.011	0.015	0.022	0.013	0.017	0.022	0.045	0.06	0.077	0.007
	1.99	0.22	0.25	0.30	0.040	0.046	0.055	0.031	0.034	0.038	0.11	0.122	0.134	0.009
	3.26	0.47	0.62	0.93	0.086	0.11	0.17	0.047	0.053	0.063	0.165	0.19	0.23	0.008

Table S6: Results of the parameter search using the two-subunit CaMKII autophosphorylation model. Values of normalized (and real) probability  $r_{\alpha}^{(0)}$  ( $r_{\alpha}$ ), and  $k_{eff}^{PP}$  for one-phospho and two-phospho rates 2-subunit CaMKII autophosphorylation models that provided the best fit to the experimental data are given for different temperature and free Ca<sup>2+</sup>. The lower and upper limits of parameter  $r_{\alpha}^{(0)}$  that provided acceptable fits are given in columns min and max respectively. In the case of the two-phospho rates variant, the normalized parameter  $k_{ap}^{P(0)}$  was 0.05 s<sup>1/2</sup> (25°C) and 0.10 s<sup>1/2</sup> (30°C),. Real probability  $r_{\alpha}$  was obtained using the fast phosphorylation values of  $k_{aa}^P$  given in Table 5. In the one-phospho rates variant, two available estimates of the T286 phosphorylation rate  $k_{aa}^P$  were used to define the fast (6.3/s at 25°C and 11.9 /s at 30°C) and the slow (0.53/s at 25°C and 1/s at 30°C) phosphorylation rate variants.

T286 phosphorylation 1/ $K_{\alpha 4}$ [nM] T [°C]	Two-phospho				One-phospho			
	fast		slow		fast		slow	
	20	60	20	60	20	60	20	60
	25/30	25/30	25/30	25/30	25/30	25/30	25/30	25/30
4-activation	-/-	-/-	-/-	-/-	±/-	-/-	-/-	-/-
3-activation	±/+	±/+	-/±	-/-	±/±	±/±	+ /±	-/-
2-activation	±/+	±/+	-/+	-/±	-/-	±/±	+ /+	+ /+

Table S7: Validity of different variants of the two-subunit CaMKII activation and autophosphorylation model.

Results obtained from numerical simulations of the 4, 3-4, and 2-3-4 activation variants of the Ca-CaM-CaMKII equilibrium model for two values of 1/ $K_{\alpha 4}$ , and for two values of the T286 phosphorylation rate were matched against the values of  $r_{\alpha}$  obtained for one- and two-phospho rates variants of the two-subunit CaMKII autophosphorylation model for both 25 and 30°C. “+” indicates that it was possible to find the affinity increase factors  $s_1$ -  $s_4$  so that the variant fully satisfies the constraints, “±” that it was possible to find the affinity increase factors  $s_1$ -  $s_4$  so that the variant satisfies the relaxed, but not full, constraints, and “-” that it was not possible to find the affinity increase factors  $s_1$ -  $s_4$  so that the variants satisfies the constraints.

T [ $^{\circ}$ C]	Two-phospho						One-phospho					
	25			30			25			30		
	$s_1$	$s_3$	$s_4$	$s_1$	$s_3$	$s_4$	$s_1$	$s_3$	$s_4$	$s_1$	$s_3$	$s_4$
3-act, fast, 20	1	32	2	1	32	2	3.9	2	4	6.3	2	4
3-act, fast, 60	1	32	2	1	32	2	1	4	32	3.7	4	1
3-act, slow, 20							3.6	16	1	7.9	16	1
3-act, slow, 60												
2-act, fast, 20	1	32	8	1	32	8						
2-act, fast, 60	1	32	8	1	32	8	1	8	16	1	2	32
2-act, slow, 20							1.3	22.6	4	1.4	1.4	16
2-act, slow, 60							1.4	32	1	2.2	2.8	4

Table S8: Representative values of the affinity increase factors  $s_1$ -  $s_4$  for the two-subunit model. Shown are representative examples of values of  $s_1$ - $s_4$  for all different combinations of the variants that are consistent with our experimental data. In each case, the values shown in this table lay in the middle of the range of values that are consistent with the experimental data. Whenever possible the values for 25 $^{\circ}$ C and 30 $^{\circ}$ C were chosen to be similar. Left column defines variant combinations: 3- or 2-activation, fast or slow T286 phosphorylation, and two different values of  $1/K_{\alpha 4}$  (20 or 60 nM).

## References

- Bradshaw JM, Kubota Y, Meyer T, Schulman H (2003) An ultrasensitive  $\text{Ca}^{2+}$ /calmodulin-dependent protein kinase II-protein phosphatase 1 switch facilitates specificity in postsynaptic calcium signaling. *Proc Natl Acad Sci U S A* 100: 10512–7
- Hanson PI, Meyer T, Stryer L, Schulman H (1994) Dual role of calmodulin in autophosphorylation of multifunctional cam kinase may underlie decoding of calcium signals. *Neuron* 12: 943–56
- Miller SG, Kennedy MB (1986) Regulation of brain type ii  $\text{Ca}^{2+}$ /calmodulin-dependent protein kinase by autophosphorylation: a  $\text{Ca}^{2+}$ -triggered molecular switch. *Cell* 44: 861–70